Inorg. Chem. **2006**, *45*, 9580–9586

Modulation of the Lowest Metal-to-Ligand Charge-Transfer State in $[Ru(bpy)_2(N–N)]^{2+}$ Systems by Changing the N–N from Hydrazone to Azine: Photophysical Consequences

Maria Abrahamsson and Leif Hammarström

Chemical Physics, Department of Photochemistry and Molecular Science, The Ångström Laboratories, Uppsala University, Box 523, SE-751 20 Uppsala, Sweden

Derek A. Tocher

Department of Chemistry, University College London, 20 Gordon Street, London WC1H 0AJ, U.K.

Samik Nag and Dipankar Datta*

Department of Inorganic Chemistry, Indian Association for the Cultivation of Science, Calcutta 700 032, India

Received June 20, 2006

Two Ru(II) complexes, $[Ru(bpy)_2L](ClO_4)_2$ (**1**) and $[Ru(bpy)_2L'](BF_4)_2$ (**2**), where bpy is 2,2′-bipyridine, L is diacetyl dihydrazone, and L′ 1:2 is the condensate of L and acetone, are synthesized. From X-ray crystal structures, both are found to contain distorted octahedral RuN_6^{2+} cores. NMR spectra show that the cations in **1** and **2** possess a C_2 axis in solution. They display the expected metal-to-ligand charge transfer (^{1}MLCT) band in the 400–500 nm region. Complex **1** is nonemissive at room temperature in solution as well as at 80 K. In contrast, complex **2** gives rise to an appreciable emission upon excitation at 440 nm. The room-temperature emission is centered at 730 nm (λ_{em}^{max}) with a quantum yield (Φ_{em}) of 0.002 and a lifetime (τ_{em}) of 42 ns in an air-equilibrated methanol–ethanol solution. At 80 K, $\Phi_{em} = 0.007$ and $\tau_{em} = 178$ ns, with a λ_{em}^{max} of 690 nm, which is close to the 0–0 transition, indicating an ^{3}MLCT excited-state energy of 1.80 eV. The radiative rate constant (5×10^4 s^{-1}) at room temperature and 80 K is almost temperature independent. From spectroelectrochemistry, it is found that bpy is easiest to reduce in **2** and that L is easiest in **1**. The implications of this are that in **2** the lowest ^{3}MLCT state is localized on a bpy ligand and in **1** it is localized on L. Transient absorption results also support these assignments. As a consequence, even though **2** shows a fairly strong and long-lived emission from a Ru(II) → bpy CT state, the Ru(II) → L CT state in **1** shows no detectable emission even at 80 K.

Introduction

Ru(II) complexes have attracted much interest because of their interesting photophysical properties[1] and their extensive use as photosensitizers in various types of molecular assemblies. Many possible applications such as molecular electronics and light harvesting devices include photoinduced electron- and energy-transfer processes.[2] The efficiency of these processes is to a large extent dependent on the excited-state properties of the photosensitizer. Therefore, it is essential to control and tune these properties.

Ru(II)−tris(bipyridine), $[Ru(bpy)_3]^{2+}$ (bpy is 2,2′-bipyridine), is often taken as the model complex for trisbidentate Ru(II)−polypyridine complexes. Its lowest excited state is the emissive triplet metal-to-ligand charge-transfer (^{3}MLCT) state, $Ru^{III}(bpy^-)(bpy)_2$. From this long-lived ^{3}MLCT state,

* To whom correspondence should be addressed. E-mail: icdd@mahendra.iacs.res.in.

(1) Juris, A.; Balzani, V.; Barigelletti, F.; Campagna, S.; Belser, P.; von Zelewsky, A. *Coord. Chem. Rev.* **1988**, *84*, 85.

(2) (a) Barigelletti, F.; Flamigni, L. *Chem. Soc. Rev.* **2000**, *29*, 1. (b) Hagfeldt, A.; Grätzel, M. *Acc. Chem. Res.* **2000**, *33*, 629. (c) Alstrum-Acevedo, J. H.; Brennaman, M. K.; Meyer, T. J. *Inorg. Chem.* **2005**, *44*, 6802. (d) Sun, L.; Hammarström, L.; Åkermark B.; Styring, S. *Chem. Soc. Rev.* **2001**, *30*, 36.

10.1021/ic061116k CCC: $33.50
Published on Web 10/18/2006

the desired photoinduced reactions can take place. Modifying or changing any of the bipyridine ligands gives wide possibilities to tune the photophysical properties of the chromophore.[1] The orbital nature of the lowest excited state is obviously important for the excited-state properties, and most Ru(II)−polypyridyl complexes maintain the ^{3}MLCT state as the lowest one.

In heteroleptic complexes with ligands having similar lowest unoccupied molecular orbital (LUMO) energies, the differently localized ^{3}MLCT states lie close together and it may be unclear on which ligand the lowest excited state is actually localized. Despite similar energies, localization on different ligands may give rise to notably different photophysical properties. Furthermore, for assemblies in which the Ru complex is attached to an electron donor or acceptor via one of the ligands, the rate of the electron- and energy-transfer processes can change dramatically depending on whether the lowest excited state is localized on a bridging or a remote ligand.[3] Thus, it is very important to control the localization of the lowest excited state.

Herein, we report two $[Ru(bpy)_2(N-N)]^{2+}$ systems where a deliberate, slight modification of the N−N moiety induces a change from Ru(II) → N−N charge transfer to Ru(II) → bpy charge transfer as the lowest excited state. The characterizations of the corresponding MLCT states and their photophysical properties are described herein.

Results and Discussion

Systems and Their Syntheses. For the purpose of this work, the cation $[Ru(bpy)_2L]^{2+}$, where L is diacetyl dihydrazone, was chosen. Its hexafluorophosphate salt has been synthesized and characterized earlier by Vos and coworkers[4a] in 1993. However, the X-ray crystal structure of the cation $[Ru(bpy)_2L]^{2+}$ was not reported. Because several attempts to grow single crystals of $[Ru(bpy)_2L](PF_6)_2$ failed, the cation $[Ru(bpy)_2L]^{2+}$ was crystallized with ClO_4^- as a counterion. Single crystals of $[Ru(bpy)_2L](ClO_4)_2$ (**1**) can be obtained readily. Complex **1** is synthesized as red crystals in 60% yield by refluxing *cis*-$Ru(bpy)_2Cl_2\cdot 2H_2O$ with a slight excess of diacetyl dihydrazone (L) in a 1:1 (v/v) mixture of methanol and water and then adding a large excess of $NaClO_4\cdot H_2O$ to the filtered red reaction mixture. To compare the properties of **1**, we have also isolated the cation $[Ru(bpy)_2L']^{2+}$, where L′ is the 1:2 condensate of L and acetone, as a tetrafluoroborate, $[Ru(bpy)_2L'](BF_4)_2$ (**2**). We prepared **2** as a reddish-brown crystalline compound in 50% yield by refluxing *cis*-$Ru(bpy)_2Cl_2\cdot 2H_2O$, L, and acetone in a MeOH−H_2O (1:1; v/v) mixture and then adding $NaBF_4$ to the filtered reddish reaction mixture. It was not possible to synthesize L′ by reacting L with neat acetone in a dry atmosphere; the reaction has always yielded a waxlike mass that could not be characterized. Consequently, L′ was generated in situ for the synthesis of **2**. Interestingly, dihydrazone complex **1** does not react at all with acetone in the MeOH−H_2O (1:1; v/v) mixture, even under refluxing condition. This shows that, in our synthesis of complex **2**, ligand L′ is formed first, which then reacts with *cis*-$Ru(bpy)_2Cl_2\cdot 2H_2O$. To examine the generality of our synthetic protocol, we have considered using 3-pentanone instead of acetone. It is found that refluxing *cis*-$Ru(bpy)_2Cl_2\cdot 2H_2O$, L, and 3-pentanone in the MeOH−H_2O (1:1; v/v) mixture, followed by the addition of an anion like ClO_4^- or PF_6^-, yields a mixture of the complexes of the 1:1 condensate of L and 3-pentanone and the 1:2 condensate of L and 3-pentanone. It has not been possible to separate the complexes from their mixture by chromatography on silica gel or alumina. Again, **1** does not react with 3-pentanone. We have also failed to synthesize the 1:2 condensate of L and 3-pentanone separately.

Chart 1. Two Conformations of the Ligand L and a Schematic Representation of the Ligand L′ [a]

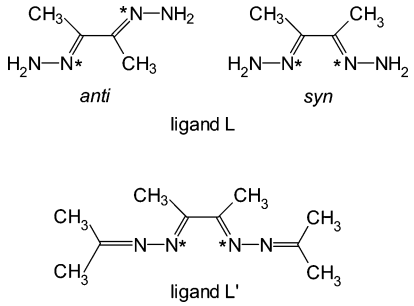

[a] The N atoms marked by asterisks bind Ru(II) here.

Crystal Structures. X-ray crystal structures of the complexes **1** and **2** have been determined. Both L and L′ are found to behave as a bidentate N,N donor ligand; the chelating fragment in both of the cases is N═C(CH_3)−C(CH_3)═N. The X-ray crystal structure of L is known.[5] It exists in the solid state in the anti form (Chart 1). In complex **1**, however, it is found to adopt the syn form (Chart 1) to bind Ru(II). Our ab initio calculations at the HF/6-31G** level using the Gaussian03 program[6] indicate that the syn

(3) (a) Kelly, L. A.; Rodgers, M. A. J. *J. Phys. Chem.* **1995**, *99*, 13132. (b) Xu, Y.; Eilers, G.; Borgström, M.; Pan, J.; Abrahamsson, M.; Magnuson, A.; Lomoth, R.; Bergquist, J.; Polivka, T.; Sun, L.; Sundström, V.; Styring, S.; Hammarström, L.; Åkermark, B. *Chem.—Eur. J.* **2005**, *11*, 7305. (c) Malone, R. A.; Kelley, D. F. *J. Chem. Phys.* **1991**, *95*, 8970.

(4) (a) Bolger, J. A.; Ferguson, G.; James, J. P.; Long, C.; McArdle, P.; Vos J. G. *J. Chem. Soc. Dalton Trans.* **1993**, 1577. (b) Euler et al.[4c] reported a weak room-temperature emission ($\Phi = 3.4 \times 10^{-4}$) from this complex, but as the emission wavelength was not significantly different from that for $[Ru(bpy)_3]^{2+}$, a minor impurity cannot be excluded as the origin of the reported emission. (c) Euler, W. B.; Cheng, M.; Zhao, C. *Polyhedron* **2001**, *20*, 507.

(5) Hauer, C. R.; King, G. S.; McCool, E. L.; Euler, W. B.; Ferrara, J. D.; Youngs, W. J. *J. Am. Chem.* Soc. **1987**, *109*, 5760.

(6) Frisch, M. J.; Trucks, G. W.; Schlegel, H. B.; Scuseria, G. E.; Robb, M. A.; Cheeseman, J. R.; Montgomery, J. A., Jr.; Vreven, T.; Kudin, K. N.; Burant, J. C.; Millam, J. M.; Iyengar, S. S.; Tomasi, J.; Barone, V.; Mennucci, B.; Cossi, M.; Scalmani, G.; Rega, N.; Petersson, G. A.; Nakatsuji, H.; Hada, M.; Ehara, M.; Toyota, K.; Fukuda, R.; Hasegawa, J.; Ishida, M.; Nakajima, T.; Honda, Y.; Kitao, O.; Nakai, H.; Klene, M.; Li, X.; Knox, J. E.; Hratchian, H. P.; Cross, J. B.; Bakken, V.; Adamo, C.; Jaramillo, J.; Gomperts, R.; Stratmann, R. E.; Yazyev, O.; Austin, A. J.; Cammi, R.; Pomelli, C.; Ochterski, J. W.; Ayala, P. Y.; Morokuma, K.; Voth, G. A.; Salvador, P.; Dannenberg, J. J.; Zakrzewski, V. G.; Dapprich, S.; Daniels, A. D.; Strain, M. C.; Farkas, O.; Malick, D. K.; Rabuck, A. D.; Raghavachari, K.; Foresman, J. B.; Ortiz, J. V.; Cui, Q.; Baboul, A. G.; Clifford, S.; Cioslowski, J.; Stefanov, B. B.; Liu, G.; Liashenko, A.; Piskorz, P.; Komaromi, I.; Martin, R. L.; Fox, D. J.; Keith, T.; Al-Laham, M. A.; Peng, C. Y.; Nanayakkara, A.; Challacombe, M.; Gill, P. M. W.; Johnson, B.; Chen, W.; Wong, M. W.; Gonzalez, C.; and Pople, J. A. *Gaussian03*, revision C.02; Gaussian, Inc.: Wallingford, CT, 2004.

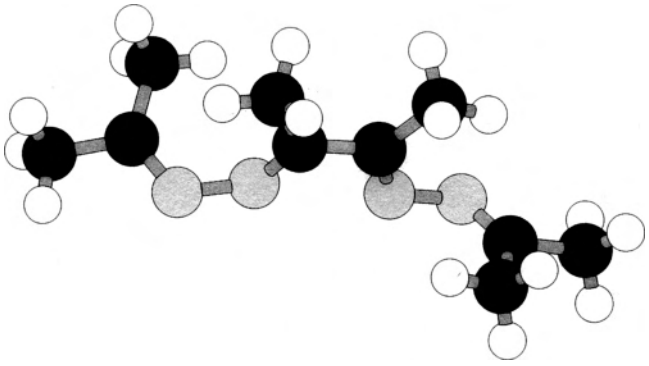

Figure 1. Ball-and-stick model of the conformation of coordinated L′ in the complex **2**. Color code: black, C; gray, N; white, H.

Table 1. Crystal Data and Refinement Parameters for the Complexes **1** and **2**

	1	**2**
formula	$C_{24}H_{26}Cl_2N_8O_8Ru$	$C_{30}H_{34}B_2F_8N_8Ru$
fw	726.50	781.34
crystal system	monoclinic	monoclinic
space group	*C*2/*c*	$P2_1/c$
a, Å	52.613(3)	19.941(3)
b, Å	10.3927(7)	9.6160(13)
c, Å	15.8084(10)	17.083(2)
α, deg	90.00	90.00
β, deg	102.6750(10)	91.662(2)
γ, deg	90.00	90.00
V, Å^3	8433.2(9)	3274.2(8)
Z	12	4
D_{calc}, g cm^{-3}	1.717	1.585
μ, mm^{-1}	0.812	0.561
θ range, deg	2.00−28.29	2.04−28.29
no. of reflns measd	36062	27397
no. of reflns used (R_{int})	10073 (0.0473)	7815 (0.0541)
no. of parameters	582	442
final R [$I > 2\sigma(I)$]		
*R*1	0.0509	0.0555
*wR*2	0.1101	0.1391
R (all data)		
*R*1	0.0717	0.0686
*wR*2	0.1189	0.1477
GOF on F^2	1.015	1.035

form of L is nonexistent in the gas phase. However, our calculations with appropriate geometric constraints reveal that the conformation of L, as found in complex **1**, is energetically less stable than the anti one in the gas phase by 11.0 kcal mol^{-1}. Many conformations are possible for the ligand L′ (Chart 1) because of the presence of four double bonds. The conformation in which L′ coordinates to Ru(II) in **2** is shown in Figure 1.

The coordination features at the metals are very similar in **1** and **2** and will be described together. Complex **2** crystallizes in the monoclinic space group $P2_1/c$ with one cation and two BF_4^- ions in the asymmetric unit, and **1** crystallizes in the space group *C*2/*c* and the asymmetric unit contains one molecule in a general position, a second molecule on the 2-fold axis at (0, *y*, 0.25), and three ClO_4^- ions. Important crystallographic parameters are listed in Table 1. An ORTEP view of the cation in complex **1** is given in Figure 2 and that of **2** in Figure 3. The geometry of the RuN_6 core in both the complexes is distorted octahedral because of the small bite of the chelating ligands. All eight Ru−N(bpy) distances reported here lie in a narrow range from 2.047(3)−2.078(3) Å. Ru−N(bpy) distances trans to the

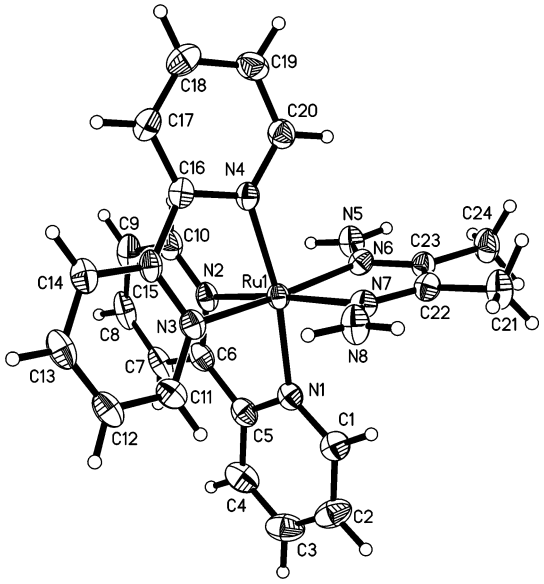

Figure 2. Structure of the cation in **1** with thermal ellipsoids and labeling scheme. Selected bond distances (Å) and angles (deg): Ru(1)−N(6) 2.030(3), Ru(1)−N(7) 2.034(3), Ru(1)−N(4) 2.052(3), Ru(1)−N(1) 2.060(3), Ru(1)−N(3) 2.066(3), Ru(1)−N(2) 2.078(3), N(6)−Ru(1)−N(7) 76.15(12), N(6)−Ru(1)−N(4) 95.86(11), N(7)−Ru(1)−N(4) 92.98(11), N(6)−Ru(1)−N(1) 91.77(11), N(7)−Ru(1)−N(1) 94.63(12), N(4)−Ru(1)−N(1) 170.32(12), N(6)−Ru(1)−N(3) 172.87(12), N(7)−Ru(1)−N(3) 99.21(12), N(4)−Ru(1)−N(3) 78.84(12), N(1)−Ru(1)−N(3) 94.02(12), N(6)−Ru(1)−N(2) 98.20(11), N(7)−Ru(1)−N(2) 171.43(12), N(4)−Ru(1)−N(2) 94.01(12), N(1)−Ru(1)−N(2) 78.96(12), N(3)−Ru(1)−N(2) 87.00(11), N(6)−C(23)−C(22)−N(7) 3.3(5).

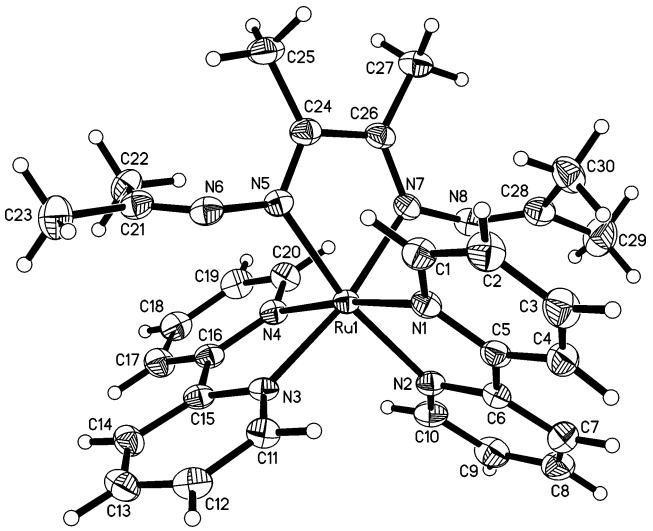

Figure 3. Structure of the cation in **2** with thermal ellipsoids and labeling scheme. Selected bond distances (Å) and angles (deg): Ru(1)−N(7) 2.030(3), Ru(1)−N(5) 2.039(3), Ru(1)−N(1) 2.047(3), Ru(1)−N(4) 2.053(3), Ru(1)−N(3) 2.062(3), Ru(1)−N(2) 2.066(3), N(7)−Ru(1)−N(5) 75.59(12), N(7)−Ru(1)−N(1) 88.35(11), N(5)−Ru(1)−N(1) 96.44(11), N(7)−Ru(1)−N(4) 96.64(11), N(5)−Ru(1)−N(4) 88.32(11), N(1)−Ru(1)−N(4) 173.84(11), N(7)−Ru(1)−N(3) 169.95(11), N(5)−Ru(1)−N(3) 95.37(11), N(1)−Ru(1)−N(3) 97.16(11), N(4)−Ru(1)−N(3) 78.45(11), N(7)−Ru(1)−N(2) 94.50(11), N(5)−Ru(1)−N(2) 169.01(11), N(1)−Ru(1)−N(2) 78.27(11), N(4)−Ru(1)−N(2) 97.69(11), N(3)−Ru(1)−N(2) 94.85(11), N(7)−C(26)−C(24)−N(5) −4.0(4), C(26)−N(7)−N(8)−C(28) 82.4(4), C(24)−N(5)−N(6)−C(21) 82.9(4), N(6)−N(5)−C(24)−C(26) 174.6(3), N(8)−N(7)−C(26)−C(24) 174.2(3).

ancillary nitrogen chelate are systematically longer than those cis to that ligand, but the differences are not statistically significant. The bonds to the unique nitrogen chelate in each

complex cation are shorter, 2.027(3)−2.039(3) Å, than those to the bipyridyl ligands. The chelate bite angles for the bipyridyl ligands are very similar, 78.27(11)−79.30(12)°, and are somewhat larger than those to the second chelate, 75.59(12)−76.96(19)°. In both complexes **1** and **2**, there are no significant deviations from planarity in the bpy rings, and the methyl groups on the backbones of the two N−N ligands are within 3° of being precisely eclipsed. Within the unique chelates in both **1** and **2**, there is some evidence of delocalized bonding. For example, in **2,** the C(24)−N(5) and C(26)−N(7) bonds, 1.288(4) and 1.291(4) Å, are slightly longer than the accepted value, 1.27 Å, for a C═N bond; in contrast, the N(5)−N(6) and N(7)−N(8) bonds, 1.407(4) and 1.405(4) Å, are a bit shorter than the conventional value of 1.46 Å for a single bond between two N atoms.

NMR and Solution Structures. From the NMR spectra of **1** and **2** in $(CD_3)_2SO$, it is revealed that the cations in them possess a C_2 axis in solution. In ^1H NMR, the two methyl groups of coordinated L in **1** are found to be magnetically equivalent; the six protons occur as a singlet at 2.33 ppm. Similar magnetic equivalence is observed for the two NH_2 groups; they resonate as a somewhat broad singlet at 6.55 ppm. The bpy protons in **1** are located in the region 7.35−8.81 ppm with the expected splitting patterns. Vos and co-workers found[4a] that the methyl protons of $[Ru(bpy)_2L](PF_6)_2$ appear as a singlet at 2.48 ppm and the NH_2 ones at 6.54 ppm in $(CD_3)_2SO$. They did not report the ^{13}C NMR spectrum of $[Ru(bpy)_2L](PF_6)_2$. In ^{13}C NMR, the methyl C's of **1** appear at 15.51 ppm. The imino C's of the coordinated L and the various bpy C's in **1** are found in the range 124.67−157.79 ppm. For discussion of the NMR spectra of **2**, we refer to Figure 3. The magnetically equivalent methyl groups on C24 and C26 (Figure 3) appear as a singlet at 2.31 ppm (cf. 2.33 ppm in **1**). The methyl groups on C21 and C28 are found to be somewhat shielded. The H atoms on C23 and C29 resonate at 0.71 ppm and those on C22 and C30 at 1.50 ppm. The bpy protons resonate in the region 7.45−8.78 ppm with the usual splitting patterns. In ^{13}C NMR, three signals are observed for the pairs (C25, C27), (C22, C30), and (C23, C29) in the region 17.20−24.33 ppm. The carbon atoms C21 and C28 appear at 166.07 ppm. Other C atoms of L′ and the bpy moieties are found in the region 124.71−162.48 ppm.

Electrochemistry. The electrochemical behaviors of **1** and **2** have been examined by cyclic voltammetry at a glassy carbon electrode in purified acetonitrile under a dry N_2 atmosphere. The voltammograms obtained at a scan rate of 50 mV s^{-1} are shown in Figure 4. Complex **1** displays irreversible oxidations at and beyond 1.23 V vs the normal hydrogen electrode (NHE). Two of the possible six ligand reductions are observed. The cathodic peak potential of the first reduction, which is irreversible, is −1.13 V vs NHE. The second ligand reduction is somewhat quasirreversible with an $E_{1/2}$ of −1.28 V vs NHE. This is in good agreement with the values reported by Vos et al.[4a] Complex **2** also gives a voltammogram similar to that for **1** with irreversible oxidations occurring at and beyond 1.29 V vs NHE. Two of the ligand redox processes in **2** are somewhat more well-

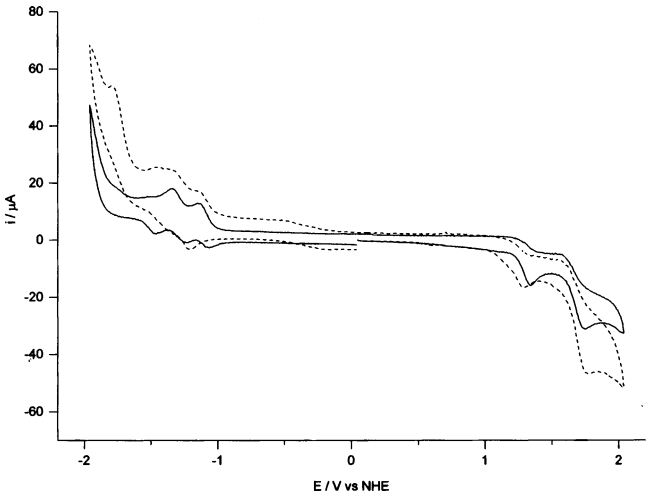

Figure 4. Cyclic voltammograms of **1** (- - -) and **2** (—) in MeCN (0.1 M in tetraethylammonium perchlorate) under a dry N_2 atmosphere at a glassy carbon electrode. Solute concentrations: **1**, 1.03 mM; **2**, 1.02 mM. Scan rate, 50 mV s^{-1}.

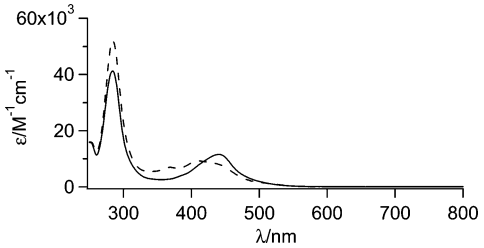

Figure 5. UV−vis spectra of **1** (- - -) and **2** (—) in acetonitrile solution.

defined with $E_{1/2}$ values of −1.11 and −1.29 V vs NHE. From these data (Figure 4), it is very difficult to say which ligand moiety is reduced first in **1** or **2**. For comparison, we mention here that, in cyclic voltammetry in MeCN at a glassy carbon electrode, $[Ru(bpy)_3]^{2+}$ shows[7] a quasirreversible oxidation [Ru(II/III) couple] with an $E_{1/2}$ of 1.51 V vs NHE with three of the possible six ligand reductions appearing as quasirreversible couples having $E_{1/2}$ values of −1.10, −1.29, and −1.54 V vs NHE. From this comparison and Figure 4, it is clear that the LUMOs in $[Ru(bpy)_3]^{2+}$ and the cations of **1** and **2** are quite close to each other in terms of energy. It is not possible to determine which ligand is the most easily reduced in **1** and **2** just from the redox data.

Electronic Absorption Spectra. UV−vis spectra of **1** and **2** in acetonitrile solution are shown in Figure 5. The complexes display the expected ^{1}MLCT band in the 400−500 nm region. The maximum of this band in **1** is blue-shifted as compared with **2**. The UV part of the spectra are dominated by the $\pi \rightarrow \pi^*$ transition in the bpy moieties centered around 288 nm for both **1** and **2**.[1,8] The extinction coefficients in the MLCT band are essentially the same for both complexes, although the transition at 288 nm is stronger in **1** compared with **2**.

(7) (a) Ji, Z.; Huang, S. D.; Guadalupe, A. R. *Inorg. Chim. Acta* **2000**, *305*, 127. (b) Tokel-Takvoryan, N. E.; Hemingway, R. E.; Bard, A. J. *J. Am. Chem. Soc.* **1973**, *95*, 6582.

(8) Sauvage, J.-P.; Collin, J.-P.; Chambron, J.-C.; Guillerez, S.; Coudret, C.; Balzani, V.; Barigelletti, F.; De Cola, L.; Flamigni, L. *Chem. Rev.* **1994**, *94*, 993.

Table 2. Emission Maximum (λ_{em}^{max}), Lifetime (τ_{em}), and Yield (Φ_{em}) and Calculated Rate Constants for Radiative (k_r) and Nonradiative Decay (k_{nr}) of **2** in the 1:4 (v/v) MeOH−EtOH Mixture

	λ_{em}^{max}/nm	τ_{em}/ns	Φ_{em}	k_r/s^{-1}	k_{nr}/s^{-1}
298 K	729	42	2×10^{-3}	5×10^4	2×10^7
80 K	690	178	7×10^{-3}	4×10^4	5×10^6

Emission Properties. All emission measurements were performed on redissolved X-ray quality crystals in a methanol−ethanol mixture (room- and low-temperature glass) or acetonitrile (room temperature). No impurity emission could be detected. Complex **1** is not emissive either at room temperature or at 80 K, as was reported by Vos and coworkers earlier.[4] In contrast, complex **2** shows an appreciable emission, at ambient temperature as well as at 80 K. The emission properties of **2** are summarized in Table 2. The room-temperature emission is centered at 730 nm, which is very red-shifted compared with $[Ru(bpy)_3]^{2+}$. The emission quantum yield and lifetime at room temperature is 2×10^{-3} and 42 ns, respectively, in air-equilibrated methanol−ethanol solution. Purging with argon to reduce oxygen quenching gives a negligible effect, as the emission lifetime is already rather short. At 80 K, the emission yield and lifetime are 7×10^{-3} and 178 ns, respectively. Ru(II)−polypyridine complexes typically display excited-state lifetimes of 1−15 μs in a 77 K glass, although they might be very short-lived (less than 1 ns) at room temperature.[1,8] The 80 K emission maximum of **2** is at 690 nm, which is close to the 0−0 transition.[9] This corresponds to an ^{3}MLCT excited-state energy of 1.80 eV, lower than that for the pivotal $[Ru(bpy)_3]^{2+}$ cation ($E_{00} = 2.12$ eV).[1] The radiative rate constant at room temperature and 80 K, as calculated from the emission quantum yields and emission lifetimes, is almost temperature independent, $k_r = 5 \times 10^4$ s^{-1}, and lies in the same range as that for many other Ru(II)−polypyridine complexes.[10]

The photophysical properties of **2** are rather different compared with other Ru(II)−polypyridine complexes, especially the excited-state lifetime and emission quantum yield at 80 K. It should be noted though, that the radiative rate constant is fairly similar to many other complexes of the same type. Thus, the results are not conclusive concerning which ligand is involved in the lowest ^{3}MLCT state, although the fact that **2** is emissive and **1** is not might indicate that different ligands are involved in the lowest excited-state localization.

Transient Absorption. Transient absorption measurements of **2** after excitation with a ca. 5 ns laser pulse at 440 nm were performed in the spectral range 350−800 nm (Figure 6). Immediately after the excitation pulse, a ground-state bleach in the MLCT band region is observed, as well as an excited-state absorption feature around 360 nm, which is typical for a formally reduced bpy ligand in the excited state.[1] A very small excited-state absorption is also seen above 600 nm. The transient spectral features are very similar to those reported for $[Ru(bpy)_3]^{2+}$.[11] The decay time constant is uniform over the whole spectral range and equals the emission lifetime, ca. 40 ns. In particular, the absorption around 360 nm and the isosbestic point at 400 nm suggest that the lowest ^{3}MLCT state is localized on a bpy moiety (vide infra).

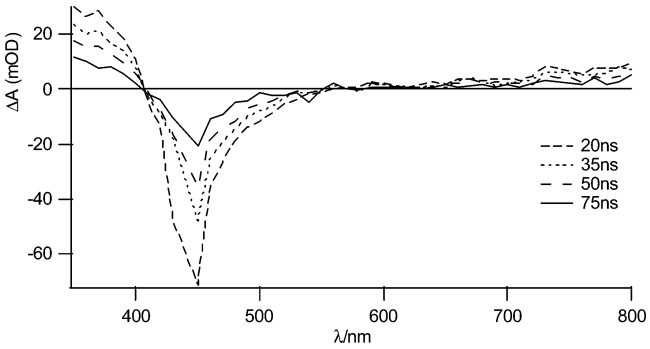

Figure 6. Transient absorption spectrum of **2** in MeCN after excitation with a ca. 5 ns laser pulse at 440 nm.

Spectroelectrochemistry. It has been pointed out above that from the electrochemical measurements it is not possible to assign the first reduction to any of the ligands in either complex. In order to determine which ligand is easiest to reduce in the complexes **1** and **2**, respectively, spectroelectrochemical measurements were performed. The samples were reduced at a potential just beyond the first reduction in the CV experiments, and the spectral changes were detected during the reduction (Figure 7). Difference spectra (final − initial) for **1** and **2** are given in Figure 8. Although very similar at first sight, there are important differences between the spectral changes for the two complexes. First, for **1**, an electrochromic shift of the bpy absorption peak at 288 nm is observed, but the intensity is almost unchanged. In contrast, for **2**, the electrochromic shift is accompanied by a decrease in peak intensity, by roughly one-third of its original intensity. This is consistent with a reduction of one of the bpy ligands in **2**. Second, the band appearing at 360 nm in **2** is typical for a reduced bipyridine, as its position is, in general, independent of the identity of the other ligands of the complex.[1] The corresponding feature in the spectrum of **1** is instead shifted to the blue. Third, the bleaching of the MLCT band is present in both complexes but is more pronounced for **2** than **1**. This is consistent with the bleach of a relatively strong Ru(II) → bpy transition in **2** but a weaker Ru(II) → dihydrazone transition in **1**. Finally, the spectrum of the reduced **2** also displays an absorption band around 510 nm, identical to the band for reduced $[Ru(bpy)_3]^{2+}$. Note that, although significant differences are observed between **1** and **2**, the results for **2** are nearly identical to those for $[Ru(bpy)_3]^{2+}$.[12]

Conclusions. From the above results it can be concluded that, in **2**, the bpy ligands are easiest to reduce. This also implies that the lowest ^{3}MLCT state is localized on a bpy

(9) (a) Treadway, J.; Loeb, B.; Lopez, R.; Anderson, P. A.; Keene, F. R.; Meyer, T. J. *Inorg. Chem.* **1996**, *35*, 2242. (b) Caspar, J. V.; Meyer, T. J. *Inorg. Chem.* **1983**, *22*, 2444.

(10) Clark, C. D.; Hoffman, M. Z.; Rillema, D. P.; Mulazzani, Q. G. J. *Photochem. Photobiol. A* **1997**, *110*, 285.

(11) Sun, H.; Yoshimura, A.; Hoffman, M. Z. *J. Phys. Chem.* **1994**, *98*, 5058.

(12) Lomoth, R.; Häupl, T.; Johansson, O.; Hammarström, L. *Chem.—Eur. J.* **2002**, *8*, 102.

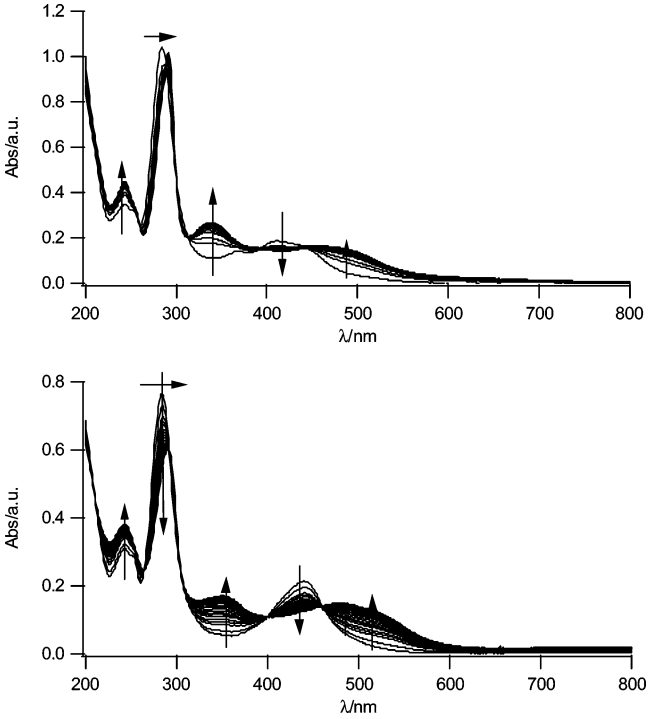

Figure 7. Spectroelectrochemistry (MeCN, 0.1 M tetrabutylammonium hexafluorophosphate). Upper panel: spectral changes upon reduction of **1** at −1.71 V vs Ag/Ag$^+$. Lower panel: spectral changes upon reduction of **2** at −1.77 V vs Ag/Ag$^+$. Arrows indicate spectral changes induced by the applied potential.

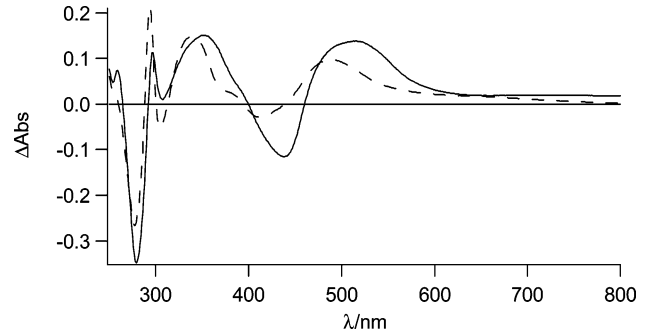

Figure 8. Difference spectrum for **1** (- - -) and **2** (—) after the first reduction in MeCN (final − initial spectra in Figure 5); normalized at 284 nm.

ligand in **2**.[1] Our transient absorption results strongly support this assignment. In contrast, the ligand easiest to reduce in **1** is the dihydrazone moiety (L), and as a consequence, the lowest ^{3}MLCT state is localized on the same ligand (i.e., L). The fact that the lowest ^{3}MLCT state is localized on different ligands in the two complexes can explain the drastic differences in emission properties. Although **2** shows a fairly strong and long-lived emission from a Ru(II) → bpy CT state, the Ru(II) → L CT state in **1** shows no detectable emission, even at 80 K.

Our present studies demonstrate that a modification of the ligand structure giving very small changes in the LUMO energy can induce large differences in the photophysical properties of these complexes. Here, an entirely nonluminescent Ru(II)N$_6$ core in a Ru−dihydrazone complex (**1**) has been turned into an emissive one in **2**, opening the door for new applications.

Experimental Section

General Information. Hydrated $RuCl_3$, $NaClO_4 \cdot H_2O$, and $NaBF_4$ were purchased from Aldrich. $Ru(bpy)_2Cl_2 \cdot 2H_2O$[13] and diacetyl dihydrazone[5] were prepared by literature procedures. Microanalyses were performed by a Perkin-Elmer 2400II elemental analyzer. UV−vis spectra were recorded either on a Hewlett-Packard 8453 instrument or on a Varian Cary 50 BIO spectrophotometer in 1 × 1 cm quartz cuvettes, Fourier transform infrared (FTIR) spectra were on a Shimadzu FTIR-8400S spectrometer, 300 MHz NMR spectra (reference: TMS) were on a Bruker DPX300 spectrometer, and electrospray ionization mass spectrometry (ES-IMS) was on a Qtof Micro YA263 spectrometer.

Synthesis of [Ru(bpy)$_2$L](ClO$_4$)$_2$ (1). *cis*-$Ru(bpy)_2Cl_2 \cdot 2H_2O$ (104 mg, 0.2 mmol) was added to L (29 mg, 0.25 mmol) dissolved in 20 mL of a degassed MeOH−H_2O (1:1; v/v) mixture, and this mixture was refluxed under a N_2 atmosphere for 8 h. It was then cooled to room temperature and filtered. To the red filtrate was added dropwise with constant stirring a solution of 1 g of $NaClO_4 \cdot H_2O$ dissolved in 3 mL of water; this mixture was then left in the air. After 1 week, the deposited red crystals, suitable for X-ray crystallography, were filtered off, washed with 5 mL of water, and dried in vacuo over fused $CaCl_2$. Yield: 90 mg (60%). Anal. Calcd for $C_{24}H_{26}N_8O_8Cl_2Ru$: C, 39.65; H, 3.61; N, 15.42. Found: C, 39.49; H, 3.78; N, 15.36. FTIR (KBr), ν/cm^{-1}: 1089 vs, 623 m (ClO_4). ESIMS (CH_3CN), *m*/*z*: 626.2 (**1** − ClO_4^-; 7%), 263.7 (**1** − 2 ClO_4^-; 100%).

Synthesis of [Ru(bpy)$_2$L′](BF$_4$)$_2$ (2). *cis*-$Ru(bpy)_2Cl_2 \cdot 2H_2O$ (104 mg, 0.2 mmol) and 3 mL of acetone were added to L (29 mg, 0.25 mmol) dissolved in 20 mL of a degassed MeOH−H_2O (1:1; v/v) mixture, and this mixture was refluxed under a N_2 atmosphere for 8 h. It was then cooled to room temperature and filtered. To the reddish-orange filtrate was added dropwise with constant stirring a solution of 220 mg (2 mmol) of $NaBF_4$ dissolved in 3 mL of water; this mixture was then left in the air. After 10 days, the reddish-brown crystalline precipitate was filtered off, washed with 5 mL of water, and dried in vacuo over fused $CaCl_2$. Yield: 80 mg (50%). Brown single crystals were grown by direct diffusion of petroleum ether into a dilute acetone solution of the complex. Anal. Calcd for $C_{30}H_{34}N_8B_2F_8Ru$: C, 46.10; H, 4.39; N, 14.34. Found: C, 46.12; H, 4.20; N, 14.20. FTIR (KBr), ν/cm^{-1}: 1120 w, 1083 vs, 528 w (BF_4). ESIMS (CH_3CN), *m*/*z*: 695.3 (**2** − BF_4^-; 8%), 304.1 (**2** − 2BF_4^-; 100%).

Crystallographic Studies of 1 and 2. Single crystals were mounted on glass fibers, and all geometric and intensity data were taken from the samples on a Bruker SMART APEX charge-coupled device (CCD) diffractometer using graphite-monochromated Mo Kα radiation (λ = 0.710 73 Å) at 150 ± 2 K. Data reduction and integration were carried out with SAINT+[14] and absorption corrections applied using the program SADABS.[15] Structures were solved by direct methods and developed using alternating cycles of least-squares refinement and difference Fourier synthesis. All non-hydrogen atoms were refined anisotropically. Hydrogen atoms were placed in geometrically reasonable positions and allowed to ride on the atoms to which they were attached. The SHELXTL PLUS V6.12 program package[16] was used to find the structure solution and for refinement.

(13) Sullivan, B. P.; Salmon, D. J.; Meyer, T. J. *Inorg. Chem.* **1978**, *17*, 3334.
(14) *Area Detector Control and Data Integration and Reduction Software*; Brüker AXS: Madison, MI, 2001.
(15) Sheldrick, G. M. *SADABS*; University of Göttingen, Göttingen, Germany, 1997.
(16) *SHELXTL PLUS V6.12*; Brüker AXS: Madison, MI, 2001.

Cyclic voltammetry was performed using an EG&G PARC electrochemical analysis system (Versastat II) under a dry nitrogen atmosphere in purified MeCN in conventional three-electrode configurations. A planar EG&G PARC G0229 glassy carbon millielectrode was used as the working electrode, and the reference electrode was Ag, AgCl/NaCl (satd). A Pt wire was used as the auxiliary electrode. Under the same experimental conditions, the ferrocene−ferrocenium (Fc/Fc^+) couple appears at 0.62 V with a peak-to-peak separation of 70 mV at a scan rate of 50 mV s^{-1}. To correct the potentials (Figure 4) to NHE, the $E°(Fc/Fc^+)$ in MeCN is taken as 0.665 V vs NHE.[17]

Steady-State Emission. Measurements were performed on a SPEX-Fluorolog II fluorometer or on a SPEX Fluorolog-3 and corrected for different detector sensitivities at different wavelengths. Measurements at 80 K were performed in a variable-temperature liquid nitrogen cryostat (Oxford Instruments), and the temperature was set with either Temperature Controller ITC601 or ITC502 from Oxford Instruments. All emission measurements were performed in 1 × 1 cm quartz cuvettes. At low temperature, a 1:4 (v/v) MeOH−EtOH mixture was used as solvent, and at ambient temperature, either a MeCN or a MeOH−EtOH mixture was used.

Time-Resolved Emission and Transient Absorption. Measurements were made with a frequency-tripled Q-switched Nd:YAG laser (from Quantel) producing <10 ns flashes. Excitation light at 440 nm was obtained in an optical parametric oscillator (OPO). The emission was detected at a right angle with a monochromator and a P928-type photomultiplier tube (PMT). The PMT output was recorded on a Hewlett-Packard digital oscilloscope (2 Gsamples/s) and analyzed with a nonlinear least-squares algorithm with the Applied Photophysics LKS60 software. Excited-state lifetimes at 77 K were measured in a liquid nitrogen filled coldfinger dewar. Room-temperature measurements were carried out in 1 × 1 cm quartz cuvettes. For transient absorption measurements, a pulsed Xe lamp was used as the probe light source.

Spectroelectrochemical Measurements. These were carried out in an OTTLE-type quartz cell with an optical path length of 1 mm. A platinum grid with a size of 10 × 30 mm^2 and 400 meshes per cm^2 was used as a working electrode, and the reference was Ag/Ag^+ (10 mM $AgNO_3$ in dry acetonitrile). The three-electrode system was connected to an Autolab potentiostat with a GPES electrochemical interface (Eco Chemie). Solutions were prepared from dry acetonitrile (Merck, spectroscopy grade, dried with MS 3 Å) and contained 0.1 M tetrabutylammonium hexafluorophosphate (Fluka, electrochemical grade, dried at 373 K) as a supporting electrolyte. Before all measurements, oxygen was removed by bubbling the stirred solutions with solvent-saturated argon and the samples were kept under an argon atmosphere during measurements. The spectra were recorded on an HP8435 diode-array UV−vis spectrophotometer.

Acknowledgment. L.H. and M.A. acknowledge support from the Swedish Energy Agency and The Knut and Alice Wallenberg Foundation. S.N. thanks the Council of Scientific and Industrial Research, New Delhi, India, for a fellowship.

Supporting Information Available: CIF file for complexes **1** and **2**. This material is available free of charge via the Internet at http://pubs.acs.org.

IC061116K

(17) Lever, A. B. P. *Inorg. Chem.* **1990**, *29*, 1271.